Transactions of the Japan Welding Society, Vol. 23, No. 1, April 1992

Sensing and Digital Control of Weld Pool in Pulsed MIG Welding*

By Kenji OHSHIMA**, Masaki MORITA**, Kazuo FUJII**, Mitsuyoshi YAMAMOTO** and Takefumi KUBOTA***

Abstract

A basic visual robot is proposed for sensing and controlling the weld pool shape.

It has been difficult to observe the weld pool with a TV camera, since the arc light is too strong. The authors tried to make periodically the current low enough to watch clearly the weld pool with CCD (Charge Coupled Device) camera without after image.

The weld pool is recognized by taking advantage of the feature on the brightness of the weld pool and its outskirts. A personal computer calculates the weld pool width and area in real time. The authors study the transient response of the wled pool width and area.

The wedling current is determined to get a desired response of the weld pool. It is shown how to determine the digital controller characteristic. Small variations of system parameter during operation caused by the change in the base metal thickness, heat conductivity, temperature rise are allowed while the prescribed control performance is maintained.

Experiments demonstrate the good controllability of the adjustable weld pool formation with the digital controller.

Key Words: *Digital control, Pulsed MIG welding, Controlled variable, Weld pool width, Weld pool area, State equation, Controller, Image processing, CCD camera*

1. Introduction

In the automatic arc welding, it is a basically important research to control the weld pool regardless of the disturbances in the systme parameters such as variation of the base-metal thickness and so on. A visual robot is proposed in this paper for detecting and controlling the weld pool shape in pulse MIG welding, since it is effective to control the pool width by using the pulsed welding current[1),2)].

Since the molten pool is relatively dark under the bright arc, it has been difficult to observe the pool shape clearly with a TV camera[3–7)]. The authors have tried to make the current periodically low enough to watch the weld pool with the CCD (Charge Coupled Device) camera in which the after image is very small.

In the digital controller of the welding system, the welding current and speed were taken as the manipulating variables (inputs), and the pool/bead width and penetration as the controlled quantities (outputs). Because the dynamic properties of those two outputs are similar to each other when the current changes (take the approximate one-order delay system for instance, their time constants are almost the same), we have studied the control of the weld pool width to obtain a desired response of the pool shape with the stepped current.

The method to determine the average current is based on the designation of the digital controller characteristic for getting a desired response of the pool width[9),10)].

Experiments have been performed changing some system parameters like the thickness of base metal and the results verified the validity of the pool image processing and the control system.

2. CCD Camera and Welding Current Waveform

The CCD camera has 490×401 photo-sensors and requires a charge-time of 1/30s to make an image, which is composed of the video-signal of 245 lines. In 1/60s after the charge-time, the CCD camera gives the image data of 245 lines to a image processing device with 245×256 pixels. The video-signals are converted to digital signals and are fetched as a picture with shades of 16 levels to image memories.

Fugure 1(a) shows the pulse current waveforms

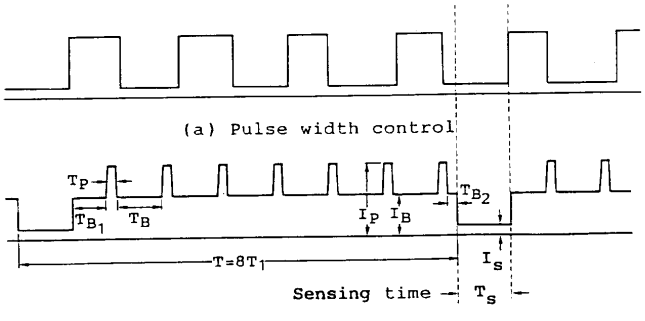

Base current: I_B, Base current duration: $T_B=30.8$ ms
Peak current: $I_P=I_B+200$A, Pulse width: $T_P=2.5$ ms
Pulse interval: $T_1=T_P+T_B$, $T_B=T_{B1}+T_{B2}$, $T_{B1}=23.1$ ms, $T_{B2}=7.7$ ms
Sensing current: $I_S=25$A, Sensing time: $T_S=T_1$

Fig. 1 Current wazeform and observation.

* Received 15 November 1991

** Department of Electrical Engineering, Saitama University, Urawa, Saitama, Japan
*** Department of Electrical Engineering, Himeji Institute of Technology, Himeji, Hyougo, Japan

against the base current duration or observation time which is more than 1/30s, the low current duration being synchronized with the sensing time of the CCD camera. Because it takes more than 0.2s to process the image and to calculate the weld pool area, we use the current waveform as shown in Fig. 1(b), and control the weld pool by adjusting the base current. In order to reduce the disturbance due to the metal transfer, taking place on account of the electrode wire being a mild steel DS1A of 1.2 mm, the current of 25A is enough to light up the weld pool in the sensing time. With the notations of Fig. 1(b), the average value of the pulsed current (I) is given by

$$I = \frac{7(I_P T_P + I_B T_B) + I_S T_S}{T} \quad [A]$$

3. Digital Control System

The system is designed as shown in Fig. 2. The video-signal in a low current duration from the CCD camera is fetched in the image memory, synchronizing with an image fetch signal (I.M.SET) produced in a timing pulse generator. A computer begins to process an image in a low current duration with an image processibg signal (SP), and calculates the current waveform so as to control the weld pool shape. This signal is given to a programmable current source through D/A converter. The pulse peak current is generated by the timing pulse (TP) in a function generator. The electrode wire is supplied in proportion to the melting rate in order to keep arc length constant.

Figure 3 shows a chart of the timing by which sensing and controlling of the weld pool are achieved. A clock pulse (CK) is produced from a vertical synchronizing signal of the video-signal.

The CCD camera can produce an image of weld pool in a period of 1/30s. However, since it takes about 0.2s to process the image and to calculate the weld pool width, we fetch a picture of weld pool into image memory every 8 periods (8/30s) of pulsed current . The sensing duration is synchronized with the sensing timing pulse (ST). In the following 1/60s, if the image set signal (I.M.SET) comes into the image

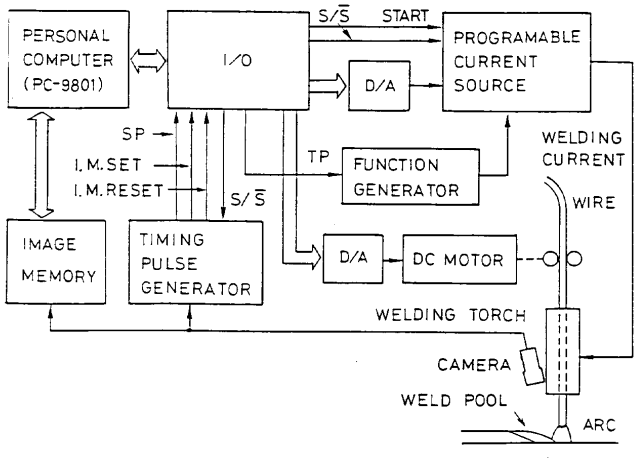

Fig. 2 Weld pool control system with CCD camera.

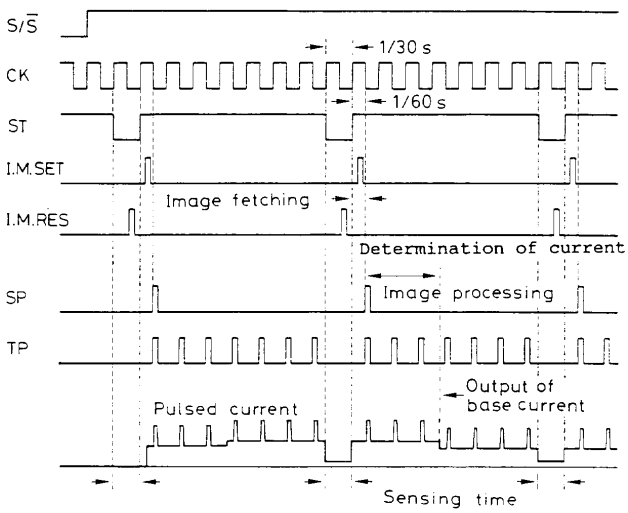

Fig. 3 Timing chart of observing weld pool and current waveform.

memories through a personal computer, the video-signals are sent to the image memory and the image remains on the memory for 7 periods until the computer finishes processing the image and determining an optimal current. Since the image is transferred to monitor TV, we can watch the weld pool in low current duration. After the video-signal of a picture is fetched to the image memory, the computer begins to calculate the weld pool width by the following sampling pulse (SP), and determines the base curren of the next pulse period so as to obtain a desired response of weld pool width. Next, the computer renews the image in the memory at the time of image reset pulse (I.M.RES). This process may be repeated.

The signal of the base current is sent to a programmable current source which is made of transistors and I.C. The current source gives a pulsed current to the electrode wire and base metal with I.M.SET pulse, when start/stop (s/s̄) signal comes with high voltage.

4. Image Processing of the Weld Pool

The weld pool image is shown in Fig. 4(a). There are slags floating near both sides of the center of the pool. Fig. 4(b) gives the distribution of the average brightness in 10 pixels along the center line AD, which almost corresponds to the temperature. The points A, B, C, D in Fig. 4(b) correspond to those in Fig. 4 (a). The point C in Fig. 4(a) corresponds to the boundary of the pool.

Furthermore, while the welding current was cut off immediately after the image of Fig. 4(a) had been fetched, the weld pool and the torch cup could be seen as in Fig. 4(c). Then , the image like Fig. 4 (d) would appear when the torch cup had been taken off.

Firstly, to recognize the pool boundary, the number of pixels of each brightness level are calculated in Fig. 4(b). When the brightness level increases in the lower level CD, the number of the pixels of the level decreases or is almost equal. However, when the

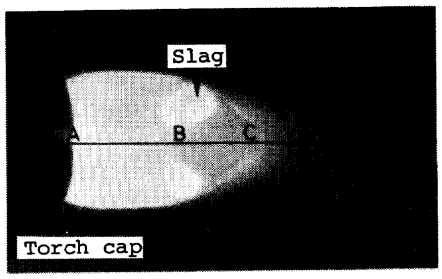

(a)

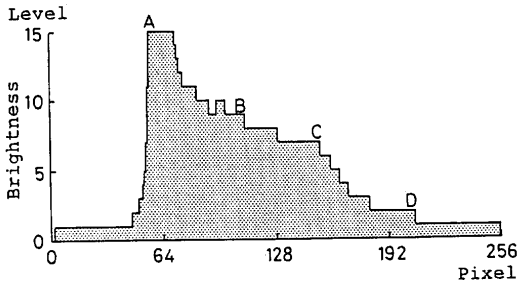

(b)

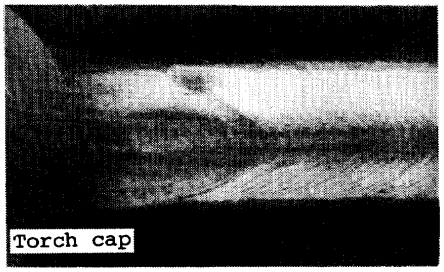

(c)

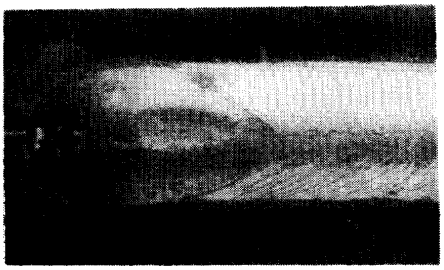

(d)

Fig. 4 Weld pool image and the distribution of brightness of about 10 pixels lines in the center of the image.

brightness level reaches the pool level, the number of pixels of the level increases.

Various pool images have been taken with differnet welding currents changed from 150A to 210A, and the spapes of the weld pool image have been compared with those of the actural pools as shown in Fig. 4(d). As the reslut, it seems that in the pool boundary, the number of pixels of the brightness level is more than 1.5 times that of the one degree lower level. It can be supposed that the lowest level of the pool brightness will be in the places where the number of pixels of the level becomes first more than 1.5 times that of one degree lower level when the brightness level increases each by one degree after another, and the levels higher than that lowest one should be considered the brightness of the pool. Hence, the pool borderline can be determined by means of calculating of the number of pixes of each brightness level from the lower to the higher.

Secondly, a method is described of finding the circumference, area and width of the weld pool. We take Fig. 5 for a simplified example. Assuming that the shaded section in Fig. 5 stands for the pool zone, one piece of rectangular panel does for one pixel (0.011 mm). The horizontal and vertical directions are defined as x and y axes respectively. From the point P at the left side of the image center, the pixels are scanned parallel to x axis until the brightness reaches the pool level. Thus the position of the pixel Q (2,3) will be recorded in the memory. Fig. 6 demonstrates the order of priority of the search vector which starts clockwise at 135 degrees from the proceeding direction and rotates counter-clockwise in order of the vector priority. Scanned from the pixel Q in Fig. 5, the point R can be discovered in the direction of the search vector(1). Therefore the proceeding direction should be changed as QR, and the pixel S could be found out in search direction (6) which is the prior vector from the position R. In the same scanning manner as mentioned above, the vector RS should be taken as a new proceeding direction so that the searching procedure can be continued. The scanning trajectory goes counter-clockwise, following the pool outline as shown by the arrows, and a at [t last comes back to the first pixel Q.

During the above processing, the calculation of the maximum and minimum x volume (Xmax and Xmin) and the amount of pixels Sy (=Xmax-Xmin+1) would be carried out for each y in the weld pool (seen in the table at the right of Fig. 5). The sum of all Sy is equal to the pool area. Moreover, as some zeros

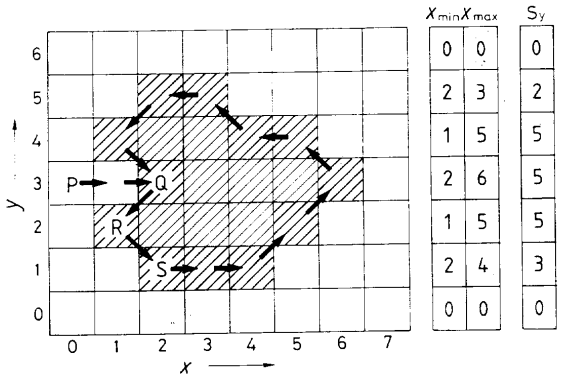

Fig. 5 Illustration of the method for calculation of the weld pool circumference, area, and width.

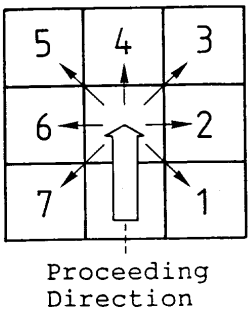

Fig. 6 Preference ranking of the search vector.

occur in the top and bottom rows of Xmax or Xmin ranked in the table of Fig. 5, the pool width can be detected according to the pixel number along the y axis.

By this method, the pool width and area can be computed with one dimension scanning, and the image processing time would be saved. Though the processing periods will not be the same due to different pool images, in Fig. 4(a) for instance, the processing time is 45 ms with one dimension scanning, but 234 ms with two dimension scanning . The former takes about 1/5 time of the latter.

It is wellknown that the wire position relative to the weld pool depends upon the welding speed. In these experiments the speed was fixed at 25 cm/min so the wire was near the front pool edge, and a part of image was hidden by the torch cup as shown in Fig. 4(a). The projection of the torch cup on the pool approximates a sector, the center point of which is located directly under the wire.

For estimating the precision of such kind of image processing, the images corresponding to Fig. 4(a) and (d) were obtained as the welding current was changed from 150A to 210A. When the pool in Fig. 4(a) was compared with the crater in Fig. 4(d), the results from the processing had errors within 3.2% and 8.5% respectively in the pool width and area.

5. State Equation of the Weld Pool

We consider a case in which the weld pool width is controlled by the base current of pulse current. The weld pool phenomena depend on the welding current waveform, arc length and welding rate[1]. We used the current waveform shown in Fig. 1(b), and kept the arc length about 5 mm by changing the wire feed rate according to the welding current. The welding rate was 25 cm/min.

First, the weld pool shape was observed in steady state. The relationship between the average value of the current I and the weld pool width W is illustrated in Fig. 7. The area and penetration characteristic of weld pool are also shown in the same figure. The base metal is a mild steel (SS41) of 4.5 mm in thickness, 100 mm in width and 500 mm in length.

The pool width increases in proportion as the average current I increases. When the current I becomes more than 150A, the slag divides the weld pool into two parts, one is front part, another is rear part wihch grows big with an increasing of the current I.

We next investigate the transient state. Figure 8 shows the transient response of the weld pool to a step input which changes from 158A to 193A at 19s after the arc statrs. It is observed that, as soon as the current increases in step function, the front part of the weld pool expands over the rear part, and it grows gradually big as illustrated in Fig. 8. Thus the response of the weld pool width takes the form

$$W = W_1(1-e^{\lambda t})+W_0$$

where W_0 is the initial value and W_1+W_0 is final

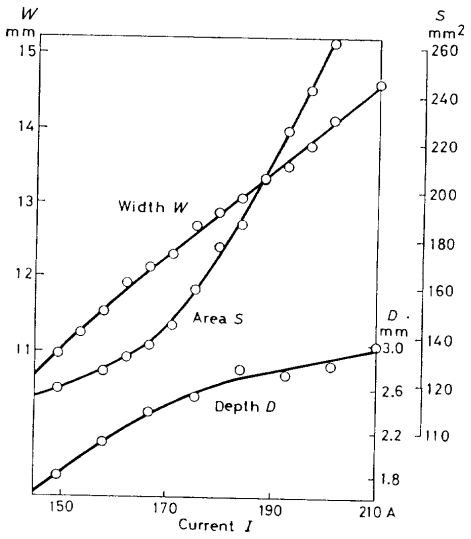

Fig. 7 Relationship among weld pool, area, penetration and current in the steady state (base metal thickness: 4.5 mm).

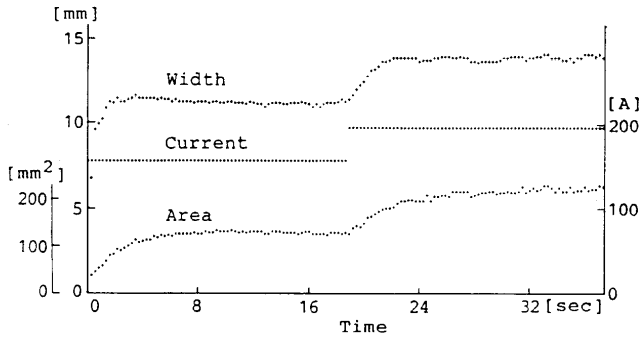

Fig. 8 Transient response of weld pool width and area.

value of the weld pool.

Linearization gives the state equation

$$\frac{dW(t)}{dt} = -\lambda W+bI-c \tag{1}$$

where b and c are coefficients which are determined by the experimental result of Fig. 7. In the responses of the weld pool to various step currents, we have

$$\lambda = 0.83/s \tag{2}$$

for a wide range of the currnet I.

In order to investigate the transient response of weld pool when the current is changed, we consider small variations u and x from the equilibrium state I_0 defined by

$$I = I_0+u, \qquad W = x \tag{3}$$

Substituting Eq.(3) into Eq.(1) gives the state equation

$$\frac{dx(t)}{dt} = -\lambda x(t)+bu(t) \tag{4}$$

where $b=0.050\ mm/(A\cdot s)$.

6. Process Controller

A schematic diagram of the weld pool width control system is shown in Fig. 9(a). At each sampling instant, the digital controller samples the error signal $e(t)$. The controller operates on this sampled value $e^*(t)$ and previous sampled values to obtain an output $u^*(t)$. This value of $u^*(t)$ is then retained until a new value is computed at the next sampling instnat.

It is likely that the CCD camera takes a weld pool picutre at the instant $t=kT$ $(k=0,1,2,...)$ the duration of Fig.9(b). Since it takes about 0.1s to calculate the weld pool area, we control the base current of welding current at one half sampling period $T_D=(1/2T)$ after the weld pool sensing. Therefore, the control system has a time delay element e^{-sT_D}. Because we use the pulsed current as illustrated in Fig.1(b), it may be assumed that the weld pool phenomena depend on the average value of the welding current, and the current waveform may be approximated by the waveform shown in Fig.9(b).

The output $u(t)$ of the zero-order hold is constant between sampling instants. That is,

$$u(t) = u(kT), \quad kT+T_D<t<(k+1)T+T_D$$

For the computer-controlled system shown in Fig.9 (a), the transfer function for the plant Eq.(4) is $b/(s+\lambda)$.

The characteristics of the digital controller are indicated by $D(z)$. The z transform for the output is

$$X(z) = \frac{G(z)D(z)R(z)}{1+G(Z)D(z)}$$

Solving for the z transform of the controller gives

$$D(z) = \frac{1}{G(z)} \frac{X(z)}{R(z)-X(z)} \tag{5}$$

This result shows that the controller characteristics $D(z)$ may be obtained by knowing the plant and zero-order hold characteristics $G(z)$ and the desired response $X(z)$ to a given input $R(z)$.

Let us determine the characteristics $D(z)$ such that the response of the system to a unit step function will be

$$\lambda(t) = 1-e^{-\alpha(t-T_D)} \tag{6}$$

where $a=0.83/s(=1/Tc)$[11]. The transfer function for the plant is $b/(s+\lambda)$, and the sampling period is $T=0.267$s.

The transfer function for the plant and zero-order hold is,

$$G(s) = e^{-sT_D} \frac{1-e^{-sT}}{s} \frac{b}{s+\lambda} \tag{7}$$

Since Eq.(7) has the time $T_D(0<T_D<t)$, we introduce

$$m = \frac{(T-T_D)}{T} = 0.5$$

Application of the modified z transform for Eq.(7) yields

$$G(z) = \frac{b}{\lambda} z^{-1} \frac{(1-e^{-m\lambda T})-(e^{-\lambda T}-e^{-m\lambda T})z^{-1}}{1-e^{-\lambda T}z^{-1}} \tag{8}$$

The z transform of a unit step input $r(t)=1$ is

$$R(z) = 1+z^{-1}+z^{-2}+... = z/(z-1)$$

The z transform of the desired response $x(t)=1-e^{-\alpha t}$, $(a=0.5/s)$ is,

$$X(z) = \frac{1}{z-1} - \frac{z}{z-e^{-\alpha T}}$$

Substitution of the preceding result into Eq.(5) gives the pulsed transfomr for the digital controller

$$D(z) = \frac{U(z)}{E(z)} = \frac{a_0+a_1z^{-1}+a_2z^{-2}}{1+b_1z^{-1}+b_2z^{-2}+b_3z^{-3}} \tag{9}$$

where

$$\begin{aligned} a_0 &= \frac{\lambda}{b}\frac{C_1}{C_2}, \quad a_1 = \frac{\lambda}{b}\frac{C_3-C_0C_1}{C_2} \\ a_2 &= -\frac{\lambda}{b}\frac{C_0C_3}{C_2}, \quad b_1 = -\frac{C_2+C_4-C_2C_3}{C_2} \\ b_2 &= \frac{C_4-C_2C_3-C_3C_4}{C_2}, \quad b_3 = \frac{C_3C_4}{C_2} \\ C_0 &= e^{-\lambda T}, \quad C_1 = 1-e^{-\alpha T/2}, \quad C_2 = 1-e^{-m\lambda T} \\ C_3 &= e^{-\alpha T/2}-e^{-\alpha T}, \quad C_4 = e^{-\lambda T}-e^{-m\lambda T}. \end{aligned} \tag{10}$$

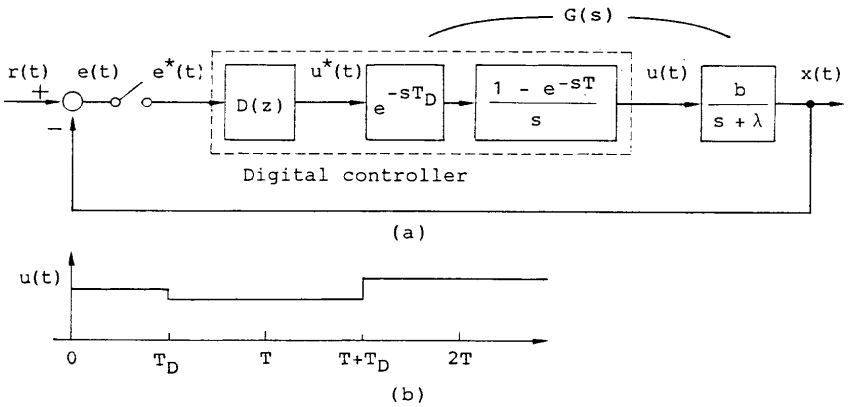

Fig. 9 Digital process controller for weld pool control (a) and base current waveform (b).

and $E(z)$ and $U(z)$ are the z transforms of input $e^*(t)$ and output $u^*(t)$ of the digital controller respectively.

The descrete form of this z transform (9) yields the desired controller characteristic

$$u(k)+b_1u(k-1)+b_2u(k-2)+b_3u(k-3) = a_0e(k)+a_1e(k-1)+a_2e(k-2) \quad (11)$$

or, by virtue of Eq. (3) and (11), this leads to

$$I(k) = a_0e(k)+a_1e(k-1)+a_2e(k-2) -b_1I(k-1)-b_2I(k-2)-b_3I(k-3) \quad (12)$$

this is the desired relationship for the digital controller which results in the desired responses for the system. The base current has been controlled in this paper.

7. Experimental Results

(1) To study the transient response characteristic of the controller, an experiment has been done with the stepped reference of the weld pool width. In the experiment an SS41 type steel plate of 4.5 mm thickness was used as the base metal and the welding speed was set at 25 cm/min. The reference was changed from 120 pixel (11.5 mm) to 140 pixels (13.4 mm) at the time of the 70 th sampling period (18.7s). According to the equation (12) the welding current was calculated out in the each sampling duration to control the weld pool. The experimental result is illustrated in Fig. 10 where the reference is drawn as a thinner line. The result well matched the desired transient response in the formula (6) as it reached 63% of the target value in 5 periods (about 1.3s) after the reference was stepped up and the steady error was very small. The variations of the current and the pool area are also represented in Fig. 10.

Being controlled after the reference was varied, the steady pool area became 182 mm^2 corresponding to the current 200A, hence there is 28% error compared with the steady area in Fig. 7 which is 253 mm^2. This error is due to the heat conductivity which is greatly affected by the change of the contacting condition between the workpiece and its supporter.

(2) Though the feed-back control is mainly used to avoid the disturbance, the control performance of the above digital controller was investigated while the characteristic of the controlled system such as the thickness of the base metal was changed.

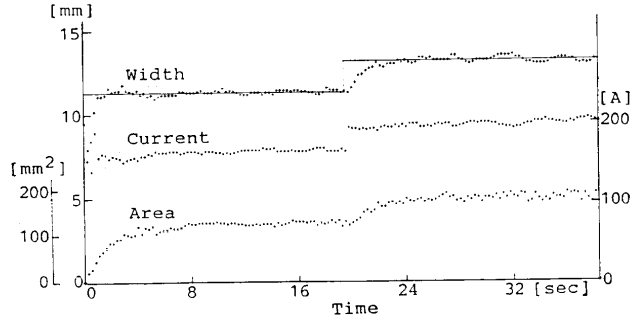

Fig. 10 Time response of weld pool width, the reference varying from 11.5 mm to 13.5 mm.

As shown in Fig. 11, the thickness of the base metal was reduced from 4.5 mm to 3.5 mm in the middle section with 80 mm longitude. The welding was carried out to form a bead-on-plate with a speed of 25 cm/min to examine the response of the weld pool width and penetration.

The response of the pool width and area to a fixed current of 165A is displayed in Fig.11(a). The average pool width is 121 pixels (11.6 mm) in the zone of 4.5 mm thick base metal but 129 pixels (12.3 mm) in the 3.5 mm thick part, which is an increase of about 7%. Fig. 11(b) exhibits a good response of the pool width and area while the welding current was controled with the width target volume of 120 pixels (11.5 mm). The width is almost kept at 120 pixels except a little changing in the narrow range when the thickness of base metal is varied.

In the case of using a constnat current (Fig.11(a)), the weld pool area in the thinner part of base metal is 2 times as large as that in the thicker part. It indicates that the cooling rate changes strongly with the variation of the plate thcikness. meanwhile, the increment of the pool area is only 40% in the thinner section of the workpiece because the current was decreased to obtain a constant pool width (Fig.11 (b)), thus improving the changing of the cooling rate.

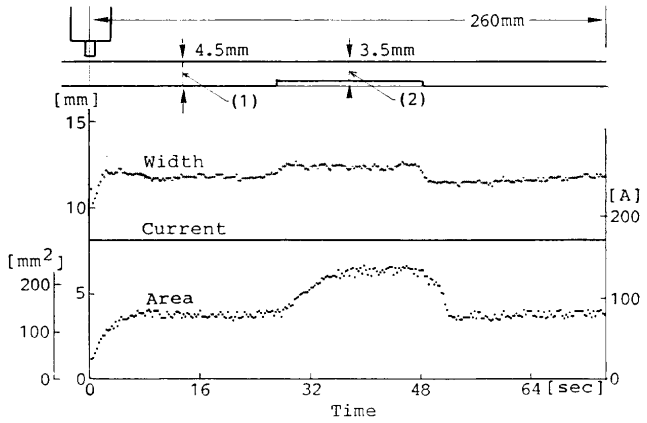

Fig. 11(a) Time response of weld pool width, the parameters varying and current being constant.

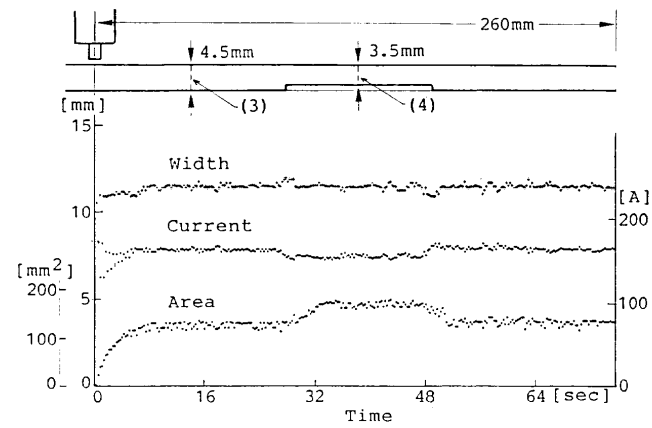

Fig. 11(b) Time response of weld pool width, the current being controlled.

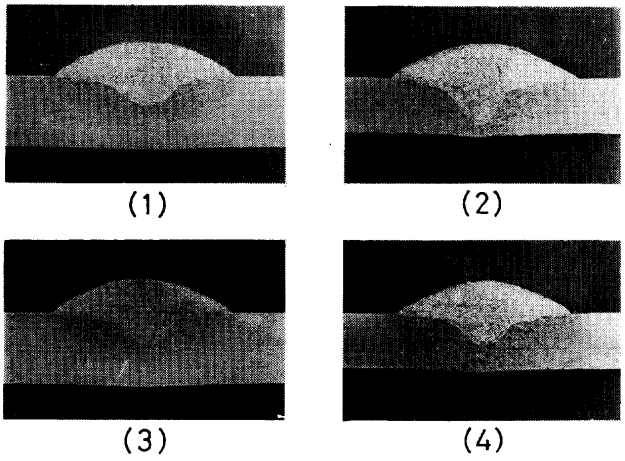

Fig. 12 Penetration shapes in positions (1)-(4) in Fig. 11(a) and (b). (1), (2); when the constat current is applied, (3), (4); when the weld.

The penetrations at the positions numbered (1), (2) in Fig.11(a) and (3),(4) in Fig.11(b) are respectively shown in pictures (1),(2),(3) and (4) in Fig.12. With a constant current, the penetration is 3.1 mm in the part of 3.5 mm thickness and is 1.9 mm in the part of 4.5 mm thickness, i.e. the former is 63% deeper than the latter. However, when the pool width is kept constant, the average current applied to the thinner zone is 8.0A smaller than that to the thicker section so that the penetrations are the same degree (2.1 mm) in all the parts with different thicknesses.

8. Conclusions

With the CCD camera, the weld pool can be clearly observed at the lower current duration in pulse MIG welding. The pool width and area are calculated periodically in real time so that the pool shape can be recoginzed by taking advantage of the features on the brightness of the weld pool and its outskirts. Taking the pulse current (average value) as the input variable and the weld pool as the state variable, the authors have studied the dynamic property of the pool and found it approximates the phenomena in the one-order delay system.

A digital controller was tested to get a desired response of the pool width and an expected transient result was obtained with a small static error. When the workpiece thickness is changed and the welding current is kept constant during welding, the pool width will increase successively in the thinner part of the base metal. On the contrary· while the digital controller operates, the width of the whole bead is controlled almost to the preset volume. A small static deviation of the pool width only appears at a very narrow range where the workpiece thickness varies.

Moreover, the penetration degree is generally inversly proportional to the base-metal thickness under constant welding current. But if the pool width is held constant, the penetration can be controlled as well regardless of the change in the workpiece thickness.

Last but not the least, this research project has been financially supported by the educational committee of Japan.

References

1) H. Maruo, Y. Hirata; ',Bead Formation in Pulsed TIG Welding", J. Japan, Weld. Soc., Vol. 3 No. 2 p. 253–260.
2) K. Oshima, T. Kubota: "Qualitative Study of Metal Transfer and Weld Pool Phenomena in Pulsed MIG Welding", The 73rd Technical commission on Physics of Welding, Japan Weld. Soc., No. 83–541 (1983).
3) A.R. Vroman and H. Brandf; Feedback Control of GTA Welding Using Puddle Width Measurement, Weld. J., 55–9 (1977).
4) K. Inoue; ',Image Processing for On-Line Detection of Welding Process Improvement of Image Quality by Incorporation of Spectrum of Arc", J. Japan Weld Soc., Vol. 50, No. 11 p. 1118–1124 (1981)
5) M. Masaki; ',Seam Tracking Arc Welding Robot with Visual Sensor", Kawasaki Heavy industry Corporation Technical Report, Vol. 78 (1981).
6) K. Inoue; "On Sensors for Arc Welding Robot", J. Japan weld Soc., Vol. 51, No. 9 p. 735–741 (1982).
7) H. Nonura, T. Yoshida, T. Nishimura, M. Nakata; "Study of Weld Pool Image Processing", Preprints of The National Meeting of J.W.S. No. 38 (1986).
8) K. Ohshima, M. Yamamoto, M. Morita, Q. Li, T. Kubota; ,'Sensing and Control of Weld Pool in Pulsed MIG Weldinb by Using CCD Camera", J. Japan Weld. Soc. Vol. 4, No. 1, Symposium in Naitonal Meeting of J.W.S. (1986).
9) Francis H. Raven; „Automatic Control Engineering", Mc-Graw-Hill (1978).
10) K. Ohshima, K. Sumi, T. Kubota, N. Kitahara, ',Sampled-Data Control of Arc length and Torch Heigh Using Image Processing Device", J. Japan Weld Soc. Vol. 3, No. 4 p. 729–736 (1985).
11) K. Ohshima, M. Abe, T. Kubota; "Sampled-Data Control of Arc Length in MIG Pulsed Arc Welding", J. Japan Weld. Soc. Vol. 51, No. 8 p. 700–707 (1982).
12) Y. Takahashi; ,'Digital Control", (1985) Iwanami.